

## Observations of Deformation in Secondary Aged Aluminium Alloys

R.G. O'Donnell<sup>1</sup>, R.N. Lumley<sup>1</sup>, I.J. Polmear<sup>2</sup>

<sup>1</sup> CSIRO Manufacturing Science and Technology, Private Bag 33, Clayton South MDC, Victoria, 3169, Australia

<sup>2</sup> School of Physics and Materials Engineering, P.O. Box 69M, Monash University, Melbourne, Victoria, 3800, Australia.

Keywords: Secondary ageing, Interrupted ageing, Fracture, Failure

### Abstract

Age hardenable aluminium alloys derive their strength primarily from the interaction between dislocations and the finely dispersed precipitates formed during ageing. These alloys are commonly given a single ageing treatment at elevated temperature (T6 temper) to develop peak properties. New processes involving interrupted ageing and secondary precipitation have been shown to modify the size and density of these precipitates leading to increases in both tensile properties and toughness. Reasons for this behaviour are now being sought by comparing deformation and fracture modes in selected alloys that have been aged to a T6 temper or subjected to interrupted ageing and secondary precipitation.

### 1. Introduction

For many years multi-step ageing treatments have been used to improve the properties of various aluminium alloys. More recently, new interrupted ageing cycles have been developed to exploit the phenomenon of secondary precipitation that may occur if alloys are first underaged at an elevated temperature, quenched and held at low temperature [1-3]. One outcome of this work is that average increases of 10% have been achieved in hardness and tensile properties [3]. These changes are associated with the presence in the microstructure of precipitates that may be finer and different than those formed when the alloys are given conventional, single stage T6 tempers. Another surprising result is that these increases in strength are often accompanied by significant increases in fracture toughness whereas these properties are usually inversely related [3].

Fracture within aluminium alloys undergoing deformation is associated with the initiation, growth and coalescence of micro-voids. Micro-voids are mechanically induced and are generally attributed to particle cracking or interfacial failure between an inclusion or precipitate particle and the surrounding matrix [4,5]. Growth and coalescence of these micro-voids is resisted by plastic deformation in the vicinity of the void nucleation site.

The aim of the present work is to investigate reasons for the simultaneous increase in strength and fracture toughness, and sometimes ductility, for heat treatments that utilise interrupted ageing and secondary precipitation. For this purpose, two interrupted ageing cycles were developed for each of three commercial wrought aluminium alloys and the microstructural changes occurring during plastic deformation have been compared with those observed when the alloys have been aged to the respective T6 tempers.

## 2. Experimental

The three commercial alloys were 2001, 6061 and 7050, and their compositions and solution treatment conditions are shown in Table 1. For the T6 temper, the alloys were aged to peak hardness at 177°C for 2001 and 6061, and 130°C for 7050. The two interrupted ageing cycles were as follows:

- Underage at the temperatures used for the T6 treatment, quench, and hold at or slightly above ambient temperature for secondary precipitation to occur (termed T6I4 where I=interrupted [1]);
- As for a), then return to a temperature equal to or close to the initial elevated temperature and age to peak hardness (termed T6I6 where I=interrupted [2]).

Table 1: Composition and solution treatment conditions for the alloys examined in this work

Alloy	Composition	Solution treatment conditions
2001	Al-5.6Cu-0.38Mg-0.33Mn-0.2Si-0.2Ti	12h at 530°C, then cold water quench
6061	Al-1Mg-0.6Si-0.3Cu	1h at 540°C, then cold water quench
7050	Al-6.2Zn-2.2Mg-2.3Cu-0.1Zr	1h at 485°C, then cold water quench

Tensile and chevron notch toughness specimens were prepared from each alloy according to the requirements of standards AS1391-1991 and ASTM E1304-97 respectively. Fracture toughness specimens were tested in the S-L orientation and tensile samples in the longitudinal orientation. Fracture surfaces were examined using scanning electron microscopy. Cross sections were prepared normal to the fracture surfaces, polished and examined un-etched by optical microscopy. In addition to examining along the gauge lengths, areas of 7.8mm<sup>2</sup> in 10 fields of view were analysed quantitatively for each specimen, that were located within 2mm and 1mm respectively from the fracture surfaces of the tensile and chevron notch specimens. Special attention was paid to measuring the number, average sizes and total areas of internal micro-voids using Image Pro Plus software.

## 3. Results and Discussion

### 3.1 Mechanical Properties

The tensile and fracture properties of the alloys in the three different temper conditions are shown in Table 2. Whereas the 0.2% proof stress of alloy 2001 was similar for each temper, tensile strength and ductility were significantly increased following the two interrupted ageing treatments. Toughness values for 2001 were similar for the T6 and T6I4 tempers and moderately (8%) higher for the T6I6 temper. For 6061, interrupted ageing caused significant increases in 0.2% proof stress, tensile strength and toughness when compared with values for the T6 temper. For example, the 0.2% proof stress for the T6I4 temper was 13% higher and the fracture toughness increased by 17%, whereas the T6I6 temper displayed a proof stress 12% higher, and the fracture toughness was increased by as much as 60%. For alloy 7050, the T6I4 treatment reduced the 0.2% proof stress by 3.5% but increased fracture toughness from 37.6MPa√m to 52MPa√m (38%). With the T6I6 treatment, 0.2% proof stress and toughness were both increased (by 5% and 9% respectively).

### 3.3 Microscopy

Results of the analysis of average sizes of the internal voids, their numbers and total areas in the 7.8mm<sup>2</sup> regions that were examined adjacent to fracture surfaces of each alloy are summarised in Table 3.

Table 2: Tensile and fracture properties of the alloys studied.

Alloy	Temper	0.2%proof stress (MPa)	UTS (MPa)	Elongation (%)	K1c (MPa√m)
2001	T6	265	376	14	56.8
	T6I4	260	420	23	56.9
	T6I6	268	414	29	61.4
6061*	T6	267	318	13	36.8
	T6I4	302	341	16	43.2
	T6I6	299	340	13	58.4
7050	T6	546	621	14	37.6
	T6I4	527	626	16	52
	T6I6	574	639	13	41.1

\* Plane strain fracture not possible for alloy 6061.

Table 3: Void characteristics in the region adjacent to fracture surfaces.

Alloy	Temper	Average void size	Number	Total void area
2001	T6	12.5μm <sup>2</sup>	113	1413μm <sup>2</sup>
	T6I4	19.2μm <sup>2</sup>	297	5699μm <sup>2</sup>
	T6I6	18μm <sup>2</sup>	543	9779μm <sup>2</sup>
6061	T6	12.4μm <sup>2</sup>	178	2209μm <sup>2</sup>
	T6I4	14.3μm <sup>2</sup>	209	2982μm <sup>2</sup>
	T6I6	40.4μm <sup>2</sup>	173	6981μm <sup>2</sup>
7050	T6	17.6μm <sup>2</sup>	65	1146μm <sup>2</sup>
	T6I4	16.7μm <sup>2</sup>	352	5894μm <sup>2</sup>
	T6I6	15.2μm <sup>2</sup>	179	2725μm <sup>2</sup>

**2001:** Figures 1a-c show optical micrographs of cross-sections prepared within the necked region of tensile specimens in the T6, T6I4 and T6I6 tempers. The deformation and fracture characteristics of the T6I4 and T6I6 tempers were similar with both exhibiting slip bands that were absent in the T6 material. Also, isolated internal cracks and microvoids were observed in the T6I4 and T6I6 specimens throughout the entire elongated gauge lengths, which was also absent in the T6 condition. Examples are shown arrowed in Figures 1b&c.

Examination revealed that the average size of voids produced in the T6I4 and T6I6 tensile specimens were each approximately 50% larger than for the T6 condition (Table 3). The numbers of voids increased from 113 (T6) to 297(T6I4) and 543 (T6I6), and the areas

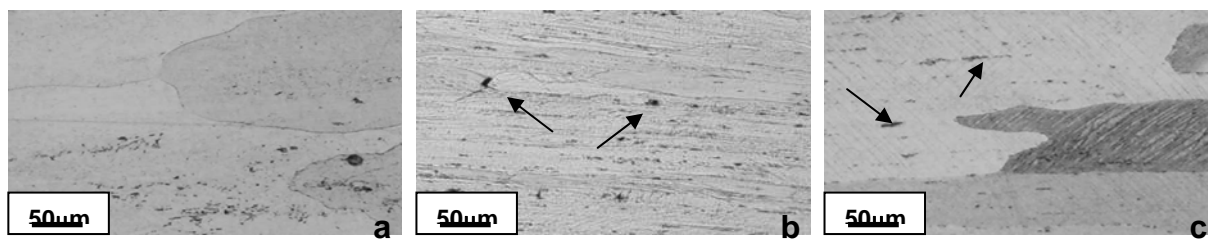


Figure 1: Cross-sections of tensile gauge lengths in the neck area for alloy 2001 after testing in (a), the T6 condition, (b) the T6I4 condition, and (c), the T6I6 condition.

increased similarly being approximately four times and seven times greater for the two interrupted ageing conditions. As shown in Figure 2, there was also a linear relationship

between void area and elongation to failure. These results indicate that the T6I4 and T6I6 tempers cause large increases in the numbers of voids and a moderate increase in their sizes. Another observation was that shear banding occurred around voids and micro-cracks suggesting that intense localised deformation had occurred there.

Figures 3a-c shows the tensile fracture surfaces of the specimens examined, which exhibit ductile dimple rupture in all three conditions. For the T6 condition, many of the dimples present showed fractured intermetallic particles at the dimple base (arrowed in Figure 3a). The average dimple size was significantly larger than for either the T6I4 or the T6I6 samples (Figures 3b&c respectively). In contrast, the samples exhibiting the largest failure strain (T6I4 and T6I6), also had relatively smoother fracture surfaces. The average sizes of the dimples were notably smaller, with fewer large dimples appearing as the elongation to failure increased. These micrographs suggest that, with the T6 sample, fracture has occurred by the coalescence of voids that form at the sites of large intermetallic particles. On the other hand, the influence of voids associated with large intermetallic particles is much less evident on the fracture surfaces of the T6I4 and T6I6 samples, which may account for their higher ductilities.

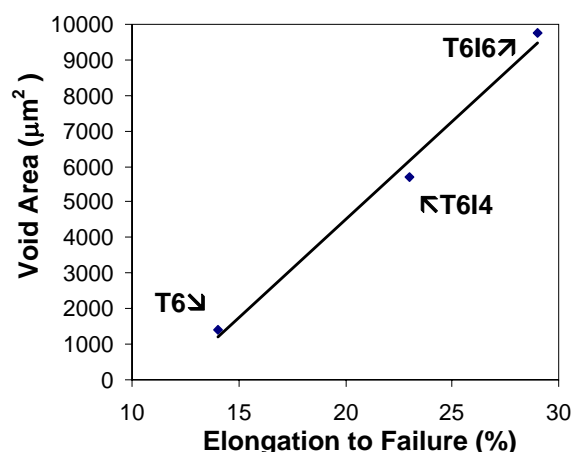


Figure 2: Analysis of micro-void area for 7.8mm<sup>2</sup> adjacent to the fracture zone in alloy 2001, for each of the three tempers examined as a function of the elongation to failure. As the elongation at failure increases, the void area increases.

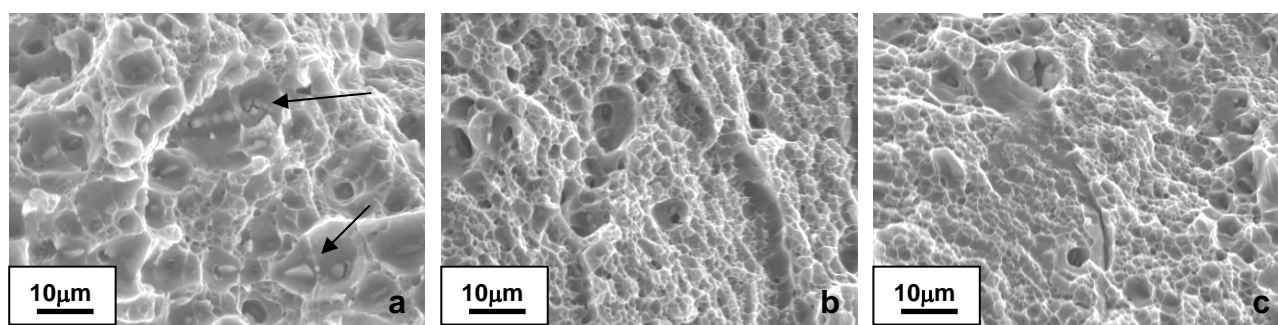


Figure 3: Tensile fracture surfaces for alloy 2001 in a) the T6 condition, b) the T6I4 condition and c) the T6I6 condition.

**6061:** Figure 4 shows the fracture surfaces of the chevron notch samples, which exhibit dimple-type rupture for all three conditions. The extent of surface relief correlated with respective values of fracture toughness, being greatest for the T6I6 temper. Observations of the 'sub-surface' micro-voids in sections of the fracture specimens revealed that whereas the number of micro-voids in each of the three tempers was generally similar (slightly higher for the T6I4 condition), the average size of these was much larger for the T6I6 specimen. In contrast to alloy 2001, the T6I6 temper has resulted in void growth during deformation rather than a significant increase in void number. In this case, a linear relationship was observed between void area and fracture toughness (Figure 5).

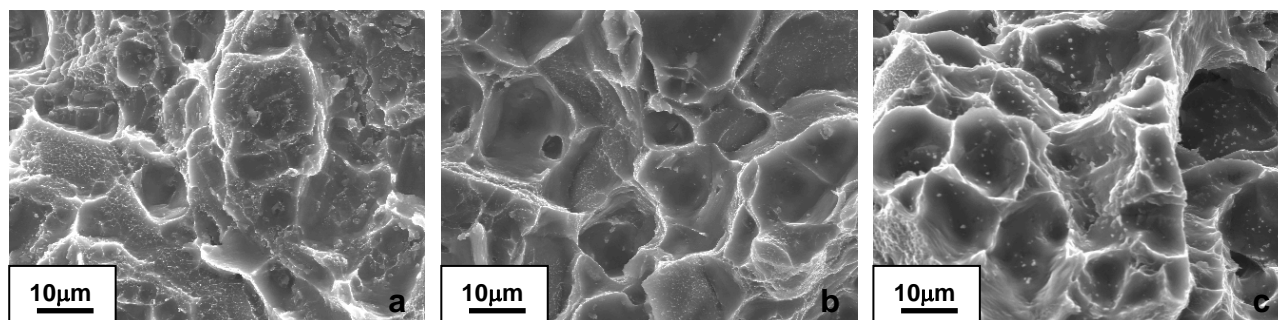


Figure 4: Chevron notch fracture surfaces for alloy 6061 in (a) the T6 condition, (b), the T6I4 condition and (c) the T6I6 condition.

**7050:** Examination of the fracture surfaces of the toughness specimens revealed a high proportion of intergranular cracks together with discontinuous steps between different grains (Figure 6, arrowed in c). This stepped surface is shown for the T6 specimen together with some evidence of micro-void coalescence (arrowed in (a)). The T6I6 specimen (Figure 6c) had a similar appearance whereas there was more evidence of ductile ligaments between the micro-voids in the T6I4 specimen (arrowed in Figure 6b). As shown in Table 3, the effects of the T6I4 and T6I6 tempers was broadly similar to the 2001 alloy in that the number of voids increased compared with that present in the T6 specimen, whereas the average size was unchanged. However, in this case, the T6I4 temper resulted in approximately double the number of voids as compared to the T6I6 specimen. Furthermore there was some similarity with 6061 in that 7050 showed a linear relationship between void area and fracture toughness (Figure 7).

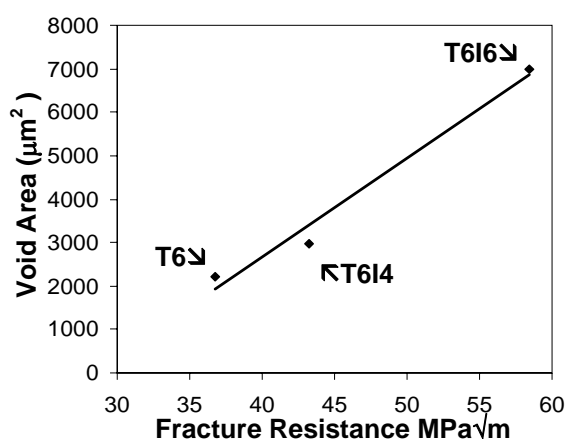


Figure 5: Void area for samples taken from nearest 1mm of material adjacent to the fracture surface for alloy 6061. The void area in the fractured samples increases simultaneously to the fracture resistance.

#### 4. Conclusions

Although the loads imposed in the tensile and fracture toughness tests have generated voids and micro-cracks in the microstructures of all alloys aged to each of the three tempers, there are significant differences in behaviour. Whereas the interrupted ageing treatments usually result in large increases in the total area of voids, this process occurs primarily from a greater number of voids in alloys 2001 and 7050, and from an increase in void size in 6061. Linear relationships exist between void area and levels of ductility in 2001 and fracture toughness in 6061 and 7050. Although the T6I6 temper is more effective than T6I4 in increasing fracture toughness in 2001, and more particularly 6061, the reverse is true for 7050.

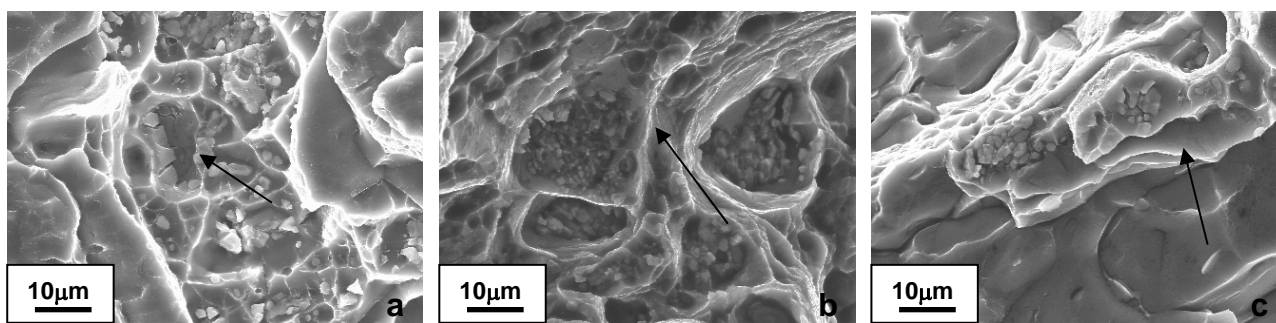


Figure 6: Chevron notch fracture surfaces for alloy 7050 in (a), the T6 condition, (b) the T6I4 condition, and (c) the T6I6 condition.

The differences in ductility and toughness resulting from these temper treatments must be related to subtle changes in microstructure, and more particularly to the size and number density of the respective precipitate dispersions. These variables will effect localised deformation, which in turn will control the formation, growth and eventual coalescence of the voids leading to fracture. The behaviour observed would seem to indicate that the simultaneous increase in tensile properties and fracture toughness may result from achieving greater homogeneity of plastic flow during deformation which delays void coalescence. Further studies are needed to elucidate the precise mechanisms involved.

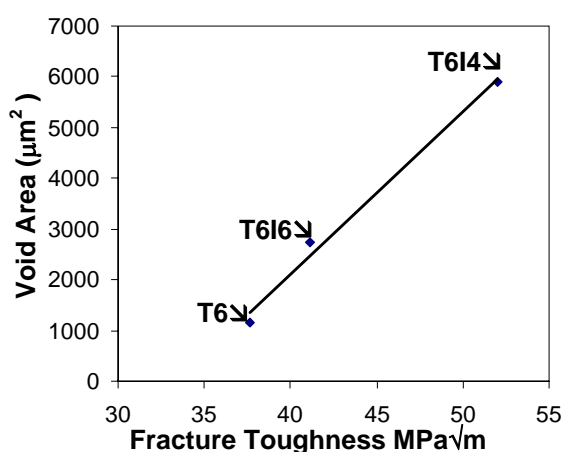


Figure 7: Void area for samples taken from nearest 1mm of material adjacent to the fracture surface for alloy 7050. The void area of the fractured samples increases simultaneously to the fracture resistance.

### Acknowledgements

The authors would like to thank CSIRO Manufacturing and Infrastructure Technology for providing funding for this work.

### References

1. R.N. Lumley, I.J. Polmear and A.J. Morton, International Patent Application PCT/AU02/00234, 2002.
2. R.N. Lumley, I.J. Polmear and A.J. Morton, International Patent Application PCT/AU00/01601, 2000.
3. R.N. Lumley, I.J. Polmear and A.J. Morton, Mat. Sci. Tech., 19, 11 1483-1490, 2003.
4. R.W. Hertzberg, Deformation and Fracture Mechanics of Engineering Materials, 4<sup>th</sup>. Ed., John Wiley and Sons, Inc., New York, 294, 1996.
5. E.A. Starke and J.T. Staley, Prog. Aerospace Sci., 32, 131-172, 1996.